Effect of Reaction Conditions on the Properties and Behavior of Wood Cellulose Nanocrystal Suspensions

ARTICLE *in* BIOMACROMOLECULES · MARCH 2005

Impact Factor: 5.75 · DOI: 10.1021/bm049300p · Source: PubMed

3 AUTHORS, INCLUDING:

Maren Roman

Virginia Polytechnic Institute and State Univ…

32 PUBLICATIONS **1,298** CITATIONS

SEE PROFILE

Effect of Reaction Conditions on the Properties and Behavior of Wood Cellulose Nanocrystal Suspensions

Stephanie Beck-Candanedo,[†] Maren Roman,[‡] and Derek G. Gray*[,†]

Department of Chemistry, Pulp and Paper Research Centre, McGill University, Montréal, Québec, H3A 2A7 Canada, and Department of Wood Science and Forest Products, Virginia Polytechnic Institute and State University, Blacksburg, Virginia 24061

Received November 4, 2004; Revised Manuscript Received December 8, 2004

Sulfuric acid hydrolysis of native cellulose fibers produces stable suspensions of cellulose nanocrystals. Above a critical concentration, the suspensions spontaneously form an anisotropic chiral nematic liquid crystal phase. We have examined the effect of reaction time and acid-to-pulp ratio on nanocrystal and suspension properties for hydrolyzed black spruce acid sulfite pulp. Longer hydrolysis times produced shorter, less polydisperse black spruce cellulose nanocrystals and slightly increased the critical concentration for anisotropic phase formation. Increased acid-to-pulp ratio reduced the dimensions of the nanocrystals thus produced; the critical concentration was increased and the biphasic range became narrower. A suspension made from a bleached kraft eucalyptus pulp gave very similar properties to the softwood nanocrystal suspension when prepared under similar hydrolysis conditions.

Introduction

Acid hydrolysis of cellulose fibers yields highly crystalline rodlike particles through selective degradation of the more accessible material. The cellulose nanocrystals that result from this degradation are of colloidal dimensions, and when stabilized, they form aqueous suspensions, the properties and applications of which are reviewed in a recent article.[1]

Rånby and Ribi were the first to produce stable suspensions of colloidal-sized cellulose crystals by sulfuric acid hydrolysis of wood and cotton cellulose.[2,3] The nanocrystals were found to be approximately 50−60 nm long by 5−10 nm wide, which agreed with previous X-ray diffraction experiments as well as electron microscopy investigations of cellulose fibers.[3] The first electron microscopy images of the cellulose nanocrystals themselves were obtained in 1953.[4] Marchessault and co-workers in 1959 and Hermans in 1963 demonstrated that such cellulose nanocrystal suspensions displayed liquid crystalline order.[5,6] However, it was not until several decades later that Revol and co-workers showed that the aqueous cellulose nanocrystal suspensions in fact formed a stable chiral nematic liquid crystalline phase.[7]

Using acid hydrolysis, native cellulose suspensions have been prepared from a variety of sources, including bacterial cellulose,[8,9] microcrystalline cellulose,[10] sugar beet primary cell wall cellulose,[11] cotton,[12] tunicate cellulose,[13] and softwood pulp (mostly black spruce).[7,14] The hydrolysis conditions are known to affect the properties of the resulting nanocrystals. For example, a longer reaction time leads to shorter nanocrystals.[12] Different acids also affect the suspension properties: hydrochloric acid hydrolysis yields cellulose rods with minimal surface charge,[10] whereas the use of sulfuric acid provides highly stable aqueous suspensions, due to the esterification of surface hydroxyl groups to give charged sulfate groups.[2] Above a critical concentration, the rodlike shape of the charged cellulose nanocrystals leads to the formation of anisotropic liquid crystalline phases, which have been extensively studied.[5,7,12,14−17]

Table 1. Dimensions of Cellulose Nanocrystals from Various Sources

cellulose type	length	cross section
tunicate[a]	100 nm − several μm	10−20 nm
bacterial[b]	100 nm − several μm	5−10 nm by 30−50 nm
algal (*Valonia*)[c]	>1000 nm	10 to 20 nm
cotton[d]	200−350 nm	5 nm
wood[e]	100−300 nm	3−5 nm diameter

[a] References 13 and 22. [b] References 27 and 28. [c] References 29 and 30. [d] Reference 26. [e] References 14 and 26; this work.

Nanocrystal size, dimensions, and shape are also determined to a certain extent by the nature of the cellulose source. The degree of crystallinity of the cellulose within the organism, as well as the dimensions of the microfibrils, varies widely from species to species.[18,19] Thus, algal and tunicate cellulose microfibrils, which are highly crystalline,[20−23] yield nanocrystals up to several micrometers in length. In contrast, wood microfibrils, which have lower crystallinity (50−83%)[24−26] yield much shorter nanocrystals.[26] Table 1 lists the nanocrystal dimensions for various cellulose sources; cross sectional dimensions are similar to those of the microfibril. Microfibril dimensions are similar for tunicate,[13,22] bacterial,[27,28] and algal cellulose,[29,30] whereas cotton and wood microfibrils are smaller.[14,26]

There are of course important differences between the cell wall structures of hardwoods and softwoods; native softwood tracheids tend to be longer (3−4 mm) than hardwood tracheids (0.5−1.5 mm), as well as somewhat wider

* To whom correspondence should be addressed. E-mail: derek.gray@mcgill.ca. Tel: 514-398-6182.
[†] McGill University.
[‡] Virginia Polytechnic Institute and State University.

10.1021/bm049300p CCC: $30.25
Published on Web 01/12/2005

Table 2. Experimental Conditions: Reaction Time and Acid-to-Pulp Ratios

sample	pulp source	reaction time, min	acid-to-pulp ratio, mL/g
E	eucalyptus	25	8.75
S1	black spruce	25	8.75
S2	black spruce	45	8.75
S3	black spruce	45	17.5

(~35 μm vs ~20 μm, respectively).[26] Data on the difference between the dimensions of softwood and hardwood microfibrils is less accessible. It is generally accepted that in wood the cellulose molecules initially form long crystalline elements with cross-section dimensions around 2−5 nm (sometimes called elementary fibrils or protofibrils) that aggregate into larger microfibrils with lateral dimensions in the tens of nanometers. Determining the exact dimensions of cellulose microfibrils is complicated by the specific limitations of the different analytical methods used. For example, in this study, we observed microfibril widths on the surface of pulp fibers of ~70 nm, which corresponds with previous atomic force microscopy (AFM) results from Hanley and Gray[31] and also with electron microscopy results.[32] However, a much smaller cross-sectional dimension of about 3−5 nm has been observed for wood microfibrils by electron diffraction[33] and AFM measurements.[14,26,31,34] In the case of AFM, tip/sample broadening represents the main limitation, resulting in an overestimation of microfibril dimensions.

In the present study, we investigate the properties of cellulose nanocrystals obtained by hydrolysis of a softwood (black spruce) and a hardwood (eucalyptus) pulp. To our knowledge, the properties and behavior of hardwood cellulose nanocrystal suspensions have not previously been examined in detail. We also examine the effects of reaction time and acid-to-pulp ratio for suspensions of black spruce nanocrystals. Nanocrystal dimensions and surface charge are measured, and the phase separation behavior and liquid crystalline properties investigated.

Experimental Methods

Materials. Bleached softwood (black spruce, *Picea mariana*) sulfite pulp (Temalfa 93) was provided by Tembec Inc., Temiscaming, Québec. Bleached hardwood (eucalyptus, *Eucalyptus* spp.) ECF pulp was provided by Cenibra S. A., Brazil. Sulfuric acid (95−98%) for hydrolysis was purchased from Fisher Scientific. Sodium hydroxide, sodium chloride, and sulfuric acid volumetric standards for titration were purchased from Aldrich. All water used was purified (Millipore Milli-Q purification system).

Sulfuric Acid Hydrolysis. Suspensions of cellulose nanocrystals were prepared as follows. Wood pulp was ground in a Wiley mill (Thomas-Wiley Laboratory Mill model 4, Thomas Scientific, U.S.A.) to pass through a 20-mesh screen. Hydrolysis was performed at 45 °C, using 64 wt % sulfuric acid at two acid-to-pulp ratios for two reaction times (see Table 2 for details). Immediately following hydrolysis, suspensions were diluted 10-fold to stop the reaction. The suspensions were then centrifuged, washed once with water, and recentrifuged. The resulting precipitate was placed in Spectrum Spectra/Por regenerated cellulose dialysis membranes having a molecular weight cutoff of 12 000−14 000 and dialyzed against water for several days until the water pH remained constant. To achieve colloidal cellulose particles, suspensions were sonicated for 7 min at 60% output control (Vibracell sonicator, Sonics & Materials Inc., Danbury, CT), while cooling in an ice bath to avoid overheating. Finally, suspensions were allowed to stand over a mixed bed resin (Sigma-Aldrich) for 24−48 h and then filtered through hardened ashless filter paper (Whatman, 541). The final aqueous suspensions were approximately 1% concentration by weight; the concentration was increased by evaporation at ambient conditions.

Gravimetric Analysis. The concentration of cellulose in the samples was determined by weighing aliquots of the samples before and after the evaporation of water (typically, by heating for 10−15 min in an oven at 105 °C).

Atomic Force Microscopy (AFM). The size distribution of the cellulose nanocrystals was determined by AFM. Original cellulose suspensions were diluted to about 1×10^{-3} to 1×10^{-4} % concentration by weight and filtered though a 0.45-μm membrane (Schleicher & Schuell, NH). A 20-μL drop of 0.1% w/v solution of poly-L-lysine (Ted Pella, Inc.) was placed on a ~1-cm^2 piece of freshly cleaved mica for 3 min and then washed off with water, and the mica was dried. A 10-μL drop of suspension was allowed to stand on the mica for 1 min and then rinsed off with water and dried. The mica was attached to an AFM specimen disk and analyzed. Images were obtained using a NanoScope IIIa Atomic Force Microscope (Digital Instruments), using an NP tip (Digital Instruments) having a nominal spring constant of 0.12 N/m. Tips have a nominal radius in the range of 20−60 nm (given by the manufacturer). Samples were scanned in contact mode under ambient conditions at 2 Hz with scan sizes ranging from 5 to 10 μm using the J piezoelectric scanner (Digital Instruments). Particle diameters were determined using the section analysis tool provided with the AFM software (Digital Instruments, version 4.32r1). Since the nanocrystals are assumed to be cylindrical in shape, the height of the nanocrystals was taken to be equivalent to the diameter, to compensate for image widening due to the convolution of the tip and the particle. Length measurements were obtained from printouts of several height mode AFM images for each sample. The uncertainty in the AFM length measurements is about 4−7 nm, and the uncertainty in the diameter measurements, 0.2−0.5 nm. Samples of black spruce and eucalyptus pulp fibers were prepared for AFM as follows: pulp sheets were uniformly dispersed in distilled water (~0.3% w/v) by prolonged vigorous stirring. The slurry was then filtered through a 200-mesh screen. The mini-handsheet was then removed and pressed between blotting paper and Teflon disks, to yield a flat surface. When the sheet was almost dry, it was pressed with a warm steel disk between Teflon disks. Sections of the mini-handsheets were glued to metal pucks for examination on the AFM.

Phase Separation Behavior. Samples of increasing cellulose concentration were prepared from a concentrated

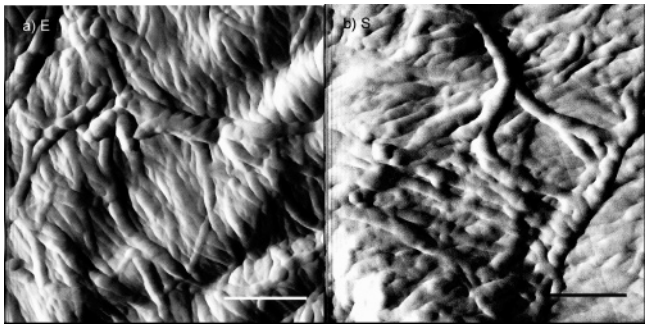

Figure 1. Deflection mode AFM images taken in air showing microfibrils on the surface of (a) eucalyptus pulp fiber and (b) black spruce pulp fiber. Scale bar = 0.5 μm.

"stock" suspension by dilution with water. Suspensions were allowed to stand for 48 h to equilibrate completely. The volume fraction of the anisotropic phase was determined by measuring the height of the lower phase in each cylindrical vial.

Conductometric Titrations. The sodium hydroxide (0.002 N) used in the conductometric titrations was standardized against carefully diluted volumetric standard sulfuric acid. A Contiburette μ10 automatic buret (Ing. CAT, Staufen, Germany) was used for all titrations. Titrations were performed with mechanical stirring and under a flow of nitrogen, using an Orion conductivity cell 018010 (cell constant $K = 0.987$ cm^{-1}) attached to a Fisher Scientific accumet pH meter 50. Sulfur content and surface charge density calculations were made using the dimensions determined by AFM, assuming a cylindrical shape and a density of 1.6 g/cm^3 for the cellulose nanocrystals.

Pitch Measurement. The chiral nematic pitch of the liquid crystalline phase was determined for each sample at a variety of total cellulose concentrations. An aliquot of each suspension was placed in a rectangular cross-section glass capillary tube having an optical path length of 0.4 mm (VitroCom Inc., NJ). Photomicrographs were taken using a polarized light microscope (Nikon Microphot-FXA), and the chiral nematic pitch was measured directly from the spacing of the fingerprint texture in the images, where the distance between the lines is equivalent to one-half the full pitch.

Results and Discussion

The effects of varying cellulose source, reaction time, and acid-to-pulp ratio were investigated for suspensions of wood cellulose nanocrystals.

Eucalyptus vs Black Spruce Cellulose. Figure 1 shows AFM deflection images of eucalyptus and black spruce pulp fiber surfaces before acid hydrolysis. For both starting materials, the cellulose microfibrils are clearly visible. The microfibril width is on the order of 70 nm and appears to be slightly ($\leq$10%) larger for black spruce than for eucalyptus. These dimensions may be influenced by AFM tip broadening artifacts but are in accord with the dimensions of aggregates of elementary fibrils.[26]

Images taken of the nanocrystals, produced from the two pulps by sulfuric acid hydrolysis, are shown in Figure 2, parts a and b. The images were used to determine the

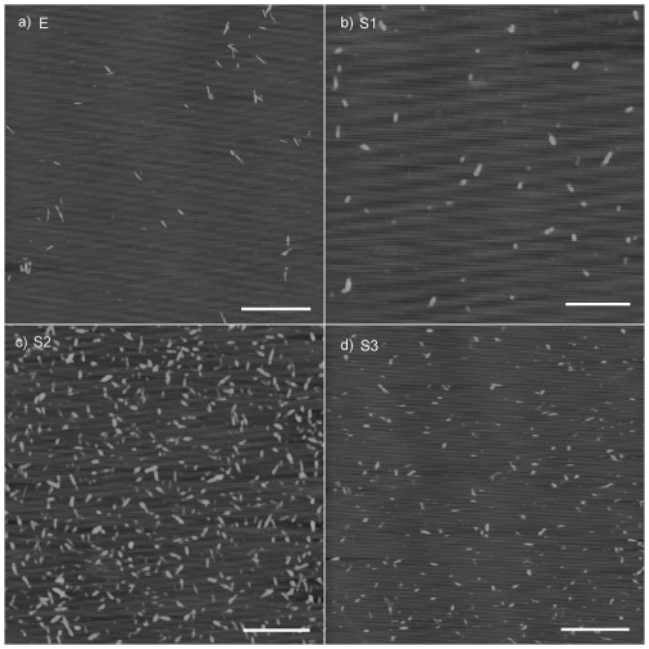

Figure 2. Height mode AFM images of cellulose nanocrystals from (a) eucalyptus pulp (E), (b) black spruce pulp (S1), (c) black spruce pulp (S2), and (d) black spruce pulp (S3). Scale bar = 1 μm. The herringbone pattern seen in the background is an artifact.

distribution of nanocrystal dimensions. Tip artifacts remain a problem in quantifying the widths of the rods, and the different apparent widths of the nanocrystals in Figure 2 may be due to the fact that different tips were used to image the black spruce and the eucalyptus samples. To eliminate the effect of tip radius on width measurements, we measured the heights of the nanocrystals, which are not subject to peak broadening artifacts, and assumed the nanocrystals to be cylindrical in shape (see Table 3 below). The cross-section dimensions of the nanocrystals clustered around 5 nm for both wood species. This is clearly smaller than the apparent size of the microfibril aggregates observed on the pulp fiber surfaces, but close to the dimensions of microfibrillar material observed in fines generated by beating spruce kraft fibers.[31]

The distribution of particle lengths in suspensions E and S1 was obtained from image analysis and is shown in Figure 3, parts a and b. The samples show a similar mean particle length and length polydispersity. The number average particle length was 147 $\pm$ 7 nm for the eucalyptus cellulose and 141 $\pm$ 6 nm for the black spruce.

As shown in Table 3, the two suspensions are essentially identical in terms of nanocrystal dimensions and surface charge, which suggests that these properties are controlled by reaction conditions such as time, temperature, and acid-to-pulp ratio, all of which were identical for the two samples. Differences in microfibril structure and size do not appear to affect the suspension properties, implying that the basic unit of wood cellulose organization is the same for the two species.

The eucalyptus and black spruce suspensions do not differ noticeably in the value of the critical cellulose concentration, c^*, required for the formation of an anisotropic liquid crystalline phase. Figure 4, parts a and b, show the phase separation diagrams of the two suspensions. The biphasic range is also essentially the same for the two pulps. Phase

Table 3. Effect of Reaction Conditions on Suspension Properties

	E	S1	S2	S3
nanocrystal length, *L*	147 ± 7 nm	141 ± 6 nm	120 ± 5 nm	105 ± 4 nm
standard deviation in *L*	65 nm	60 nm	45 nm	36 nm
nanocrystal diameter, *D*	4.8 ± 0.4 nm	5.0 ± 0.3 nm	4.9 ± 0.3 nm	4.5 ± 0.3 nm
axial ratio, *L/D*	30.6	28.2	24.5	23.3
sulfur content	0.80 ± 0.03 S%	0.89 ± 0.06 S%	1.06 ± 0.02 S%	(0.86 ± 0.02 S%)[a]
surface charge density, σ	0.29 ± 0.01 e/nm^2	0.33 ± 0.02 e/nm^2	0.38 ± 0.01 e/nm^2	—[a]
critical concentration, *c**	4.6 wt %	4.8 wt %	5.3 wt %	6.9 wt %
chiral nematic pitch, *P*[b]	21 μm	18 μm	10 μm	7 μm

[a] See text for explanation. [b] Measured at a total cellulose concentration of 7 wt %.

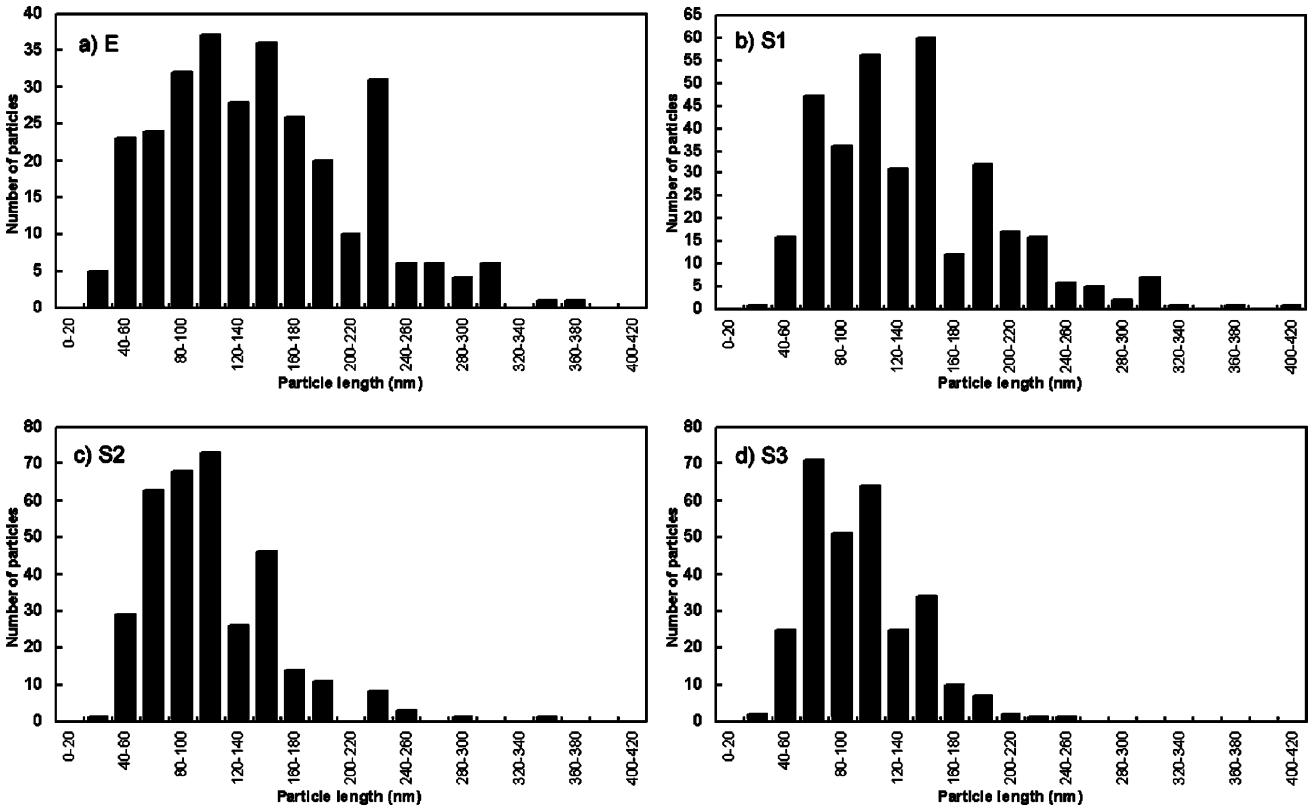

Figure 3. Distribution of particle length of cellulose nanocrystals from suspensions (a) E, (b) S1, (c) S2, and (d) S3.

separation of rodlike particles is governed by the axial ratio and the surface charge of the rods, with a decrease in either variable tending to increase the critical concentration for anisotropic phase formation.[15,35] These properties are also nearly identical for the two suspensions; there are no differences that can be attributed to the wood species.

Effect of Reaction Time on Softwood Suspension Properties. Reaction time is one of the most important parameters to consider in the acid hydrolysis of wood pulp. Too long a reaction will digest the cellulose completely to yield its component sugar molecules; too short a reaction will yield only large undispersable fibers and aggregates. There exists a fairly narrow range of reaction time which yields the desired suspension of well-dispersed colloidal nanocrystals. Within this range, the reaction time must be optimized to obtain the largest yield possible.

Black spruce pulp was subjected to 25- or 45-min hydrolysis using an acid-to-pulp ratio of 8.75 mL/g (S1 and S2, respectively). Figure 2, parts b and c, shows AFM images of the nanocrystals. The distribution of particle lengths in S2 is shown in Figure 3c. Suspension S2 shows a smaller mean particle length (120 ± 5 nm) than S1 (141 ± 6 nm), as well as a narrower, less polydisperse length distribution, attributable to the longer hydrolysis time.

Table 3 shows that at the longer reaction time, suspension S2 has a higher sulfur content. The production of shorter, less polydisperse rods with higher sulfur content at longer reaction times is consistent with previous literature results.[12,36] As expected from the larger sulfur content, the surface charge density σ of the nanocrystals, calculated using the sulfur content and the nanocrystal dimensions, appears to increase with increasing reaction time for this acid-to-pulp ratio. Suspension S1 has a surface charge density of 0.33 ± 0.02 e/nm^2, which is smaller than the value of 0.38 ± 0.01 e/nm^2 obtained for S2.

Figure 4, parts b and c, shows the phase separation diagrams for suspensions S1 and S2. Increasing the reaction time from 25 to 45 min causes an increase in the critical concentration for the formation of anisotropic phase, from 4.8 to 5.3 wt %.

According to Onsager's phase separation theory for uncharged rods, *c** decreases with increasing axial ratio

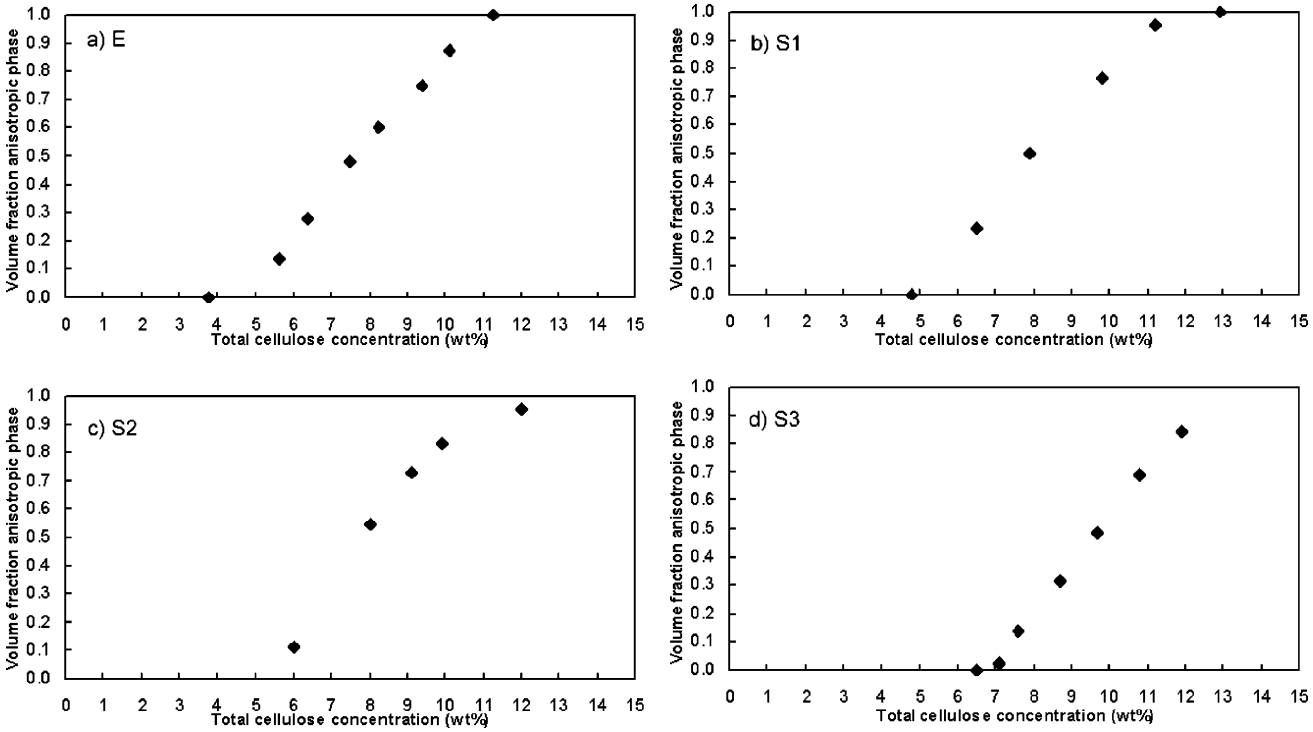

Figure 4. Phase separation diagrams for suspensions (a) E, (b) S1, (c) S2, and (d) S3. The region in which the volume fraction of the anisotropic phase, ϕ_{aniso}, lies between 0 and 1 is the biphasic region. To the left of the biphasic region, $\phi_{aniso} = 0$, and the suspensions are completely isotropic. To the right of the biphasic region, $\phi_{aniso} = 1$, and the suspensions are completely anisotropic.

(*L*/*D*).[15] However, due to the charged surface sulfate esters, the rodlike cellulose nanocrystals are polyelectrolytic in nature. The electrostatic interactions between the rods result in an increase in effective diameter and a twisting factor that governs particle orientation.[37,38] Thus, the interparticle forces are not only governed by the axial ratio but also by the ionic strength[38] and the nature of the counterions.[39] Phase separation behavior and critical concentration are very sensitive to variations in particle geometry and electrostatic interactions.[38] For example, Dong et al. found that longer hydrolysis times result in a rapid decrease in the critical concentration; more extensive hydrolysis generates cellulose rods with larger axial ratios (due to the breaking up of coarse aggregates of cellulose), as well as increased total surface charge.[12] In addition, theory predicts that the polydispersity plays a role in determining the critical concentration: The narrower length distribution of suspensions resulting from longer hydrolysis times increases the critical concentration.[40] The effect of reaction time on the critical concentrations of suspensions S1 and S2 can therefore be summarized as follows.

(1) Suspension S2 has a narrower length distribution and smaller average particle length and a slightly smaller axial ratio than S1. These factors would increase the value of c^* for S2, as observed.

(2) However, suspension S2 has a higher total surface charge (measured as sulfur content), as well as surface charge density, which would decrease the value of c^* for S2.

Based on our observations of S1 and S2, rod dimensions and geometry appear to influence critical concentration to a greater extent than surface charge in this case.

Effect of Acid-to-Pulp Ratio on Softwood Suspension Properties. Black spruce pulp was subjected to 45-min hydrolysis using acid-to-pulp ratios of 8.75 and 17.5 mL/g (suspensions S2 and S3, respectively). AFM images of the nanocrystals are shown in Figure 2, parts c and d.

The distribution of particle lengths in suspension S3 is shown in Figure 3d. Suspensions S2 and S3 show comparable mean particle lengths, the higher acid-to-pulp ratio affording a smaller mean length (120 ± 5 nm for S2 and 105 ± 4 nm for S3) as well as smaller polydispersity (Table 3).

The effect of acid-to-pulp ratio on suspension properties has not been thoroughly investigated in the literature; it has been found in this lab that larger volumes of the 64 wt % acid used tend to hydrolyze a given amount of pulp faster and thus yield shorter rods for a given reaction time. This is somewhat unexpected, as in all cases, the acid is in excess relative to the pulp. The effect is not large, as shown in Table 3: doubling the acid-to-pulp ratio resulted in a decrease in rod length of about 12.5% for a reaction time of 45 min. A recent study found the sulfur content of bacterial cellulose to increase with the acid-to-cellulose ratio and hydrolysis time.[9] The acid-to-pulp ratio was not seen to have a well-defined effect on the sulfur content of the wood cellulose suspensions (see below); suspension S3 has a lower sulfur content than S2 (0.86 vs 1.06 S%). However, it should be noted that the sulfur content listed for S3 in Table 3 was obtained using a different batch of suspension produced from the same pulp under the same reaction conditions as the suspension which was used for all other measurements.

The phase separation diagrams for suspensions S2 and S3 are shown in Figure 4, parts c and d. Doubling the acid-to-pulp ratio leads to an increase in the critical concentration (from 5.3 to 6.9 wt %). The smaller mean rod length and the lower total surface charge of the rods would also tend to increase the critical concentration of S3.

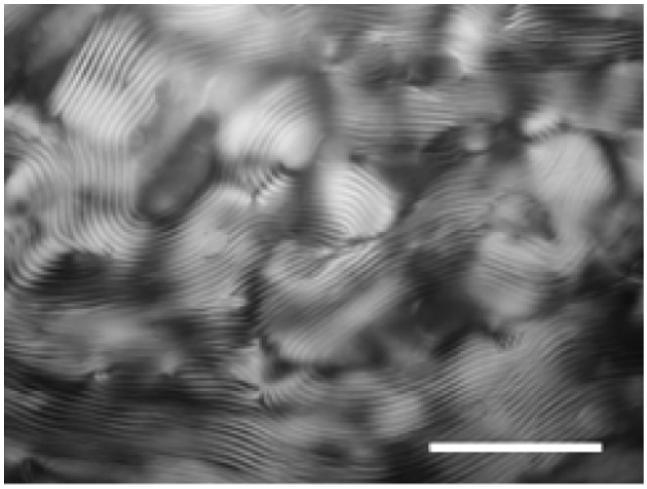

Figure 5. Fingerprint texture in chiral nematic phase of 10 wt % eucalyptus suspension, viewed in polarizing microscope. Scale bar = 200 μm. Chiral nematic pitch $P = 17$ μm.

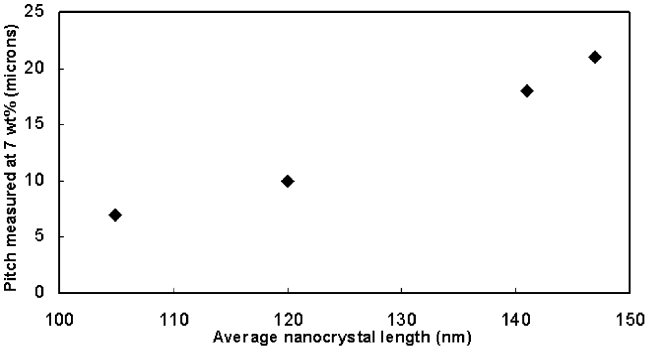

Figure 6. Effect of average cellulose nanocrystal length on the chiral nematic pitch *P* measured at 7 wt % cellulose suspension concentration.

When comparing suspensions S3 and S1, it can be seen that the combination of longer reaction time and higher acid-to-pulp ratio yields a suspension having a smaller mean rod length and narrower length distribution (i.e., smaller polydispersity), as expected. Because the critical concentration of S3 is significantly larger than that of S1, it follows that the decreases in length polydispersity affect the critical concentration to a greater extent than do decreases in average rod length under the conditions used.

Chiral Nematic Pitch. Figure 5 shows the fingerprint texture of the chiral nematic phase of a eucalyptus suspension. The chiral nematic pitch measured from the fingerprint texture in photomicrographs of the suspensions decreased with increasing cellulose concentration. For example, when S1 concentration was increased from 7 to 13 wt %, pitch decreased from ~20 to ~10 μm. This decrease in pitch with increasing concentration of chiral rods has been observed in several chiral rod systems. There are however few reports of the effect of rod length or charge on the liquid crystal chiral nematic pitch *P*. We measured the chiral nematic pitch at a total cellulose concentration of 7 wt % for all suspensions, which have varying average nanocrystal lengths. The pitch was found to increase with increasing rod length (Figure 6), in accord with an observation of Grelet and Fraden on mutant virus fd suspensions.[41] Thus, the longer rods show less tendency to form the twisted chiral nematic structure, presumably because at the same volume fraction of rods in the suspension, longer rods show a greater tendency to align in a parallel (untwisted) arrangement. The suspensions show a similar tendency to align and increase the pitch when the ionic strength is decreased.[38] The pitch found for suspensions E and S1 was close to that found for the sodium form of cotton cellulose nanocrystals by Dong and Gray at similar total cellulose concentrations.[39]

Conclusions

The properties of colloidal eucalyptus cellulose suspensions produced by sulfuric acid hydrolysis are essentially identical to those of similarly prepared black spruce cellulose suspensions. For black spruce pulp, longer hydrolysis times lead to shorter cellulose rods with narrower particle length distribution; the effect on sulfur content and surface charge is less clear. A higher acid-to-pulp ratio decreases nanocrystal dimensions to some extent at the reaction time of 45 min. At the shorter reaction time of 25 min, the effect of the acid-to-pulp ratio on critical concentration and rod dimensions may be more apparent. An effect of the reaction conditions on cellulose nanocrystal surface charge and sulfur content was not apparent. The surface charge of nanocrystals is highly sensitive to heat, as an increase in temperature can cause de-esterification of the sulfate groups on the surface of the crystals. Although we cooled the suspensions in an ice bath during sonication, an increase in temperature, in particular local temperature, cannot be completely ruled out. Surface charge and sulfur content of the cellulose may therefore be controlled by factors other than hydrolysis conditions. Chiral nematic pitch decreases with increasing cellulose concentration and decreasing nanocrystal length.

Acknowledgment. We thank NSERC for support and Dr. Nilgun Ulkem for technical assistance. S.B. thanks McGill University for a scholarship.

References and Notes

(1) de Sousa Lima, M. M.; Borsali, R. *Macromol. Rapid Comm.* **2004**, *25*, 771−787.
(2) Rånby, B. G. *Acta Chem. Scand.* **1949**, *3*, 649−650.
(3) Rånby, B. G.; Ribi, E. *Experientia* **1950**, *6*, 12−14.
(4) Mukherjee, S. M.; Woods, H. J. *Biochim. Biophys. Acta* **1953**, *10*, 499−511.
(5) Marchessault, R. H.; Morehead, F. F.; Walter, N. M. *Nature* **1959**, *184*, 632−633.
(6) Hermans, J. *J. Polym. Sci., Part C: Polym. Symp.* **1963**, *2*, 129−144.
(7) Revol, J.-F.; Bradford, H.; Giasson, J.; Marchessault, R. H.; Gray, D. G. *Int. J. Biol. Macromol.* **1992**, *14*, 170−172.
(8) Araki, J.; Kuga, S. *Langmuir* **2001**, *17*, 4493−4496.
(9) Roman, M.; Winter, W. T. *Biomacromolecules* **2004**, *5*, 1671−1677.
(10) Araki, J.; Wada, M.; Kuga, S.; Okano, T. *J. Wood Sci.* **1999**, *45*, 258−261.
(11) Dinand, E.; Chanzy, H.; Vignon, M. R. *Food Hydrocolloids* **1999**, *13*, 275−283.
(12) Dong, X. M.; Revol, J.-F.; Gray, D. G. *Cellulose* **1998**, *5*, 19−32.
(13) Favier, V.; Chanzy, H.; Cavaillé, J. Y. *Macromolecules* **1995**, *28*, 6365−6367.
(14) Araki, J.; Wada, M.; Kuga, S.; Okano, T. *Colloids Surf., A* **1998**, *142*, 75−82.
(15) Onsager, L. *Ann. N. Y. Acad. Sci.* **1949**, *51*, 627−659.
(16) Revol, J. F.; Godbout, L.; Dong, X. M.; Gray, D. G.; Chanzy, H.; Maret, G. *Liq. Cryst.* **1994**, *16*, 127−134.

(17) Araki, J.; Wada, M.; Kuga, S.; Okano, T. *Langmuir* **2000**, *16*, 2413−2415.
(18) Battista, O. A.; Coppick, S.; Howsmon, J. A.; Morehead, F. F.; Sisson, W. A. *Ind. Eng. Chem.* **1955**, *48*, 333−335.
(19) Marchessault, R. H.; Morehead, F. F.; Koch, M. J. *J. Colloid Sci.* **1961**, *16*, 327−344.
(20) Belton, P. S.; Tanner, S. F.; Cartier, N.; Chanzy, H. *Macromolecules* **1989**, *22*, 1615−1617.
(21) Sassi, J.-F.; Chanzy, H. *Cellulose* **1995**, *2*, 111−127.
(22) Terech, P.; Chazeau, L.; Cavaillé, J. Y. *Macromolecules* **1999**, *32*, 1872−1875.
(23) de Sousa Lima, M. M.; Borsali, R. *Langmuir* **2002**, *18*, 992−996.
(24) Hermans, P. H. *Makromol. Chem.* **1951**, *6*, 25−29.
(25) Sjöstrom, E. *Wood Chemistry: Fundamentals and Applications*, 2nd ed.; Academic Press: New York, 1981.
(26) Fengel, D.; Wegener, G. *Wood: Chemistry, Ultrastructure, Reactions*; Walter de Gruyter: New York, 1984.
(27) Tokoh, C.; Takabe, K.; Fujita, M.; Saiki, H. *Cellulose* **1998**, *5*, 249−261.
(28) Grunert, M.; Winter, W. T. *J. Polym. Environ.* **2002**, *10*, 27−30.
(29) Revol, J.-F. *Carbohydr. Polym.* **1982**, *2*, 123−134.
(30) Hanley, S. J.; Giasson, J.; Revol, J.-F.; Gray, D. G. *Polymer* **1992**, *33*, 4639−4642.
(31) Hanley, S. J.; Gray, D. G. *J. Pulp Paper Sci.* **1999**, *25*, 196−200.
(32) Jayme, G.; Koburg, E. *Holzforschung* **1959**, *13*, 37−43.
(33) Fink, H. P.; Hofmann, D.; Purz, H. J. *Acta Polym.* **1990**, *41*, 131−137.
(34) Harada, H.; Kishi, A.; Sugiyama, J. *Structure of cellulose microfibrils in wood*: Tsukuba: Japan, 1983; pp 6−10.
(35) Odjik, T. *Macromolecules* **1986**, *19*, 2313−2329.
(36) de Sousa Lima, M. M.; Wong, J. T.; Paillet, M.; Borsali, R.; Pecora, R. *Langmuir* **2003**, *19*, 24−29.
(37) Stroobants, A.; Lekkerkerker, H. N. W.; Odjik, T. *Macromolecules* **1986**, *19*, 2232−2238.
(38) Dong, X. M.; Kimura, T.; Revol, J.-F.; Gray, D. G. *Langmuir* **1996**, *12*, 2076−2082.
(39) Dong, X. M.; Gray, D. G. *Langmuir* **1997**, *13*, 2404−2409.
(40) Moscicki, J. K.; Williams, G. *Polymer* **1982**, *23*, 558−568.
(41) Grelet, E.; Fraden, S. *Phys. Rev. Lett.* **2003**, *90*, 198302.

BM049300P